An equivalent circuit for the Brushless Doubly Fed Machine (BDFM) including parameter estimation and experimental verification

P C Roberts* (pcr20@cam.ac.uk), R A McMahon*, P J Tavner†, J M Maciejowski*, T J Flack*
* Engineering Dept., University of Cambridge, Trumpington St., Cambridge CB2 1PZ, United Kingdom
† School of Engineering, University of Durham, Durham, DH1 3LE, United Kingdom

***Abstract*— Experimental results from a frame size 180 Brushless Doubly Fed (Induction) Machine (BDFM) fitted with four rotor designs are presented. The machine is intended for use as a variable speed generator, or drive. A per phase equivalent circuit for the machine has been developed and a method of obtaining parameters for the circuit has been described. Expressions for the torque as a function of speed have been derived and predictions of machine performance in both self-cascaded and synchronous (doubly fed) modes have been verified experimentally. The work illustrates the link between rotor equivalent circuit parameters and machine performance and a comparison between rotor designs has been made.**

NOTATION

X_1, X_2, X_r	indicating a stator 1, 2, or rotor quantity X
$\Re\{X\}, \Im\{X\}$	denotes real, imaginary part of complex X
$\angle(X)$	argument of complex X, i.e. $\arctan \frac{\Im\{X\}}{\Re\{X\}}$
R, M, L, N	resistance, mutual, self inductance, turns ratio (real)
X'	indicates an apparent (referred) quantity
P	power quantity, or parameter value
V, I	complex voltage, current
p_1,p_2	stator winding pole pairs
ω_r	BDFM rotational shaft speed
s	slip
j	$\sqrt{-1}$
$\mathbb{B}$	$\left\{ x : \begin{bmatrix} I \\ -I \end{bmatrix} x \leq \begin{bmatrix} 1 \\ \vdots \\ 1 \end{bmatrix} \right\}$, a hypercube around the origin.

Symbols may represent real or complex numbers depending on the context.

I. INTRODUCTION

The concept of incorporating two induction machines with air gap fields of different pole numbers in one frame to realize a self-cascaded machine can be attributed to Lydall [1]. Hunt also developed a machine using the same principle and showed that suitably designed stator and rotor windings could reduce copper losses significantly. Hunt's use of a single rotor winding coupling both air gap fields resulted in a more practical machine which was successful in suitable applications. These machines operated in the self-cascaded mode, that is with one stator winding fed from fixed frequency mains and the other shorted or connected to resistances [2], [3].

The advent of sources of variable voltage and frequency from inverters offered the possibility of operation in a doubly-fed mode, in which the shaft speed has a fixed relationship to the two excitation frequencies, as noted by Broadway and Burbridge [4], and subsequent work has focused on operation in this mode. Broadway and Burbridge further pointed out the attraction, from a manufacturing point of view, of a single layer rotor winding made in a similar way to normal cage windings. This design, known as the 'nested-loop' design, was adopted and refined in the work of Wallace, Spée and others who studied BDFMs of this type extensively [5]–[10]. Williamson et al. consider a machine of this type in their papers on the generalised harmonic analysis of the BDFM [11], [12].

Current interest in the BDFM is primarily as a variable speed generator for wind turbines, although the benefits of the BDFM for variable speed drives have also been demonstrated [10]. The capital installation cost is lower, due to a fractional inverter power requirement. The advantage of brushless operation is particularly valuable for off-shore wind turbine applications where maintenance costs are high.

The authors have constructed a frame size 180 machine which has been used to study control and measurement aspects of the BDFM [13]–[15]. The authors have more recently reported on the performance of alternative rotor configurations [16]. In this paper, a per phase equivalent circuit for the BDFM is developed and a method of obtaining parameters from measured torque-speed characteristics is described. The equivalent circuit is shown to predict the performance of the BDFM and illustrates how the performance depends on the equivalent circuit parameters of the machine.

II. INTRODUCTION TO BDFM OPERATION

Details of the operation of the BDFM in synchronous mode, as shown in figure 1, have been given by various authors [8], [11]. Under synchronous conditions the shaft angular velocity is related to the supply frequencies by equation (1) (see [11]) and the frequency of rotor currents is later given by equation

(5):

$$\omega_r = \frac{\omega_1 + \omega_2}{p_1 + p_2} \tag{1}$$

This leads to a definition of slips for the power and control windings in equations (2) and (3):

$$s_1 \triangleq \frac{\omega_1 - p_1\omega_r}{\omega_1} = \frac{\omega_{r_1}}{\omega_1} \tag{2}$$

$$s_2 \triangleq \frac{\omega_2 - p_2\omega_r}{\omega_2} = \frac{\omega_{r_2}}{\omega_2} \tag{3}$$

A further relationship is given in equation (4) for the so-called natural speed, that is the synchronous speed such that according to (1) the control winding is fed with DC:

$$\omega_n = \frac{\omega_1}{p_1 + p_2} \tag{4}$$

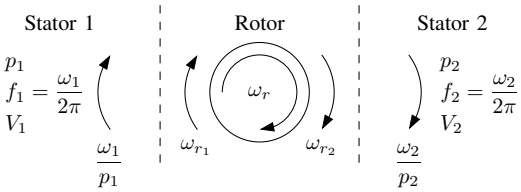

Fig. 1. BDFM synchronous mode of operation

The BDFM can also operate in the cascade mode, that is with the one winding shorted or connected to resistances. In the cascade mode the speed varies with load, but equations (1) and (5) still apply.

III. Machine Design

Table I gives the physical data for the prototype machine used throughout this and the work described in [13]–[16]. The machine is shown in Fig. 2 on the experimental test rig. Four different rotors have been constructed [16]. Rotor 1 is of 'nested-loop' design and Rotor 3 (shown in figure 3) is of a new double layer design. Both rotors have been designed for BDFM action. Rotor 2 has 18 progressive loops and Rotor 4 is a conventional cage rotor. Although these rotors do not show BDFM action, they are useful as benchmarks of performance. Details of the rotors are given in Table I.

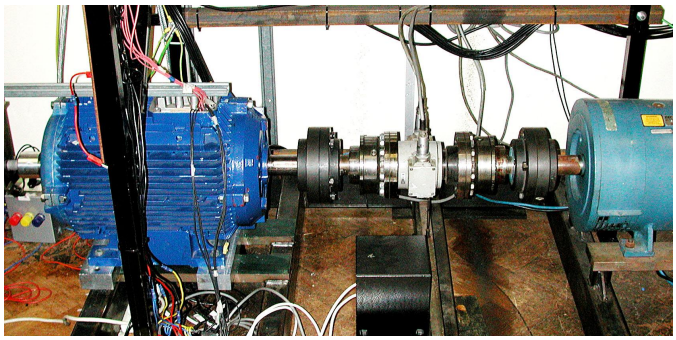

Fig. 2. Prototype BDFM machine (left) on test rig with torque transducer and DC load machine (right)

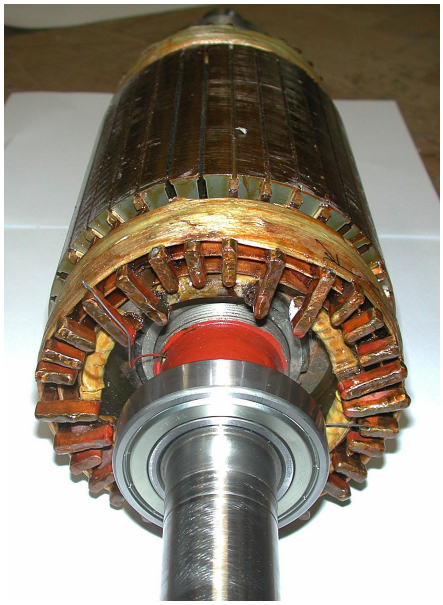

Fig. 3. Rotor 3: Prototype new double layer design

IV. Experimental Results

The aim of the experiments was to determine the torque speed characteristics of the BDFM with the different rotors to enable their performance to be compared and to provide data for the extraction of equivalent circuit parameters. Each rotor was tested in both simple induction and cascade mode. In the former case stator windings were energised in turn whilst the other was open circuit. In the latter case the non-energised stator was short-circuited. The tests were all carried out at the same reduced supply voltage of 90 Vrms (phase), 50 Hz, to limit currents to acceptable values throughout the range of the test and to avoid saturating the iron circuit. The resulting air-gap flux density was nominally 0.125 T rms for each pole number field.

The results are shown in figures 4-7 and illustrate a number of important features. All four rotors show some simple induction action, with Rotor 4 being the strongest, because it was designed for that purpose. Rotors 1 and 3, designed for BDFM action, show relatively low self-induction torques. In contrast, these rotors give strong torques in the cascade mode with the torque-speed characteristic passing through zero at the natural speed. Torques also fall to zero when the rotor is synchronous with field of the energised stator, i.e at 1500 rpm when the 4-pole winding is excited and at 750 rpm when the 8-pole field is excited. Rotors 2 and 4 do not produce torque in the cascade mode showing that negligible cross-coupling is taking place.

V. Equivalent Circuit for the BDFM

The BDFM was conceived as two distinct induction machines in the same frame, intended for operation in the self-cascaded mode. [2]. Therefore it is possible to represent the BDFM as two connected induction machines and develop an equivalent circuit using the standard per phase model.

TABLE I
PROTOTYPE MACHINE DATA

Parameter		Value
Frame size		D180
Stator core length		190mm
Stator slots		48
Stator winding 1	Poles coils per phase turns per coil	4 16 (series connected) 10
Stator winding 2	Poles coils per phase turns per coil	8 16 (series connected) 20
Effective air gap	0.5-0.6mm depending on the rotor	
Actual air gap	0.51-0.56mm depending on the rotor	
Rotor slots	36 for Rotors 1 - 3 and 40 for Rotor 4)	
Rotor 1	'Nested-loop' design of Broadway/Burbridge [4], consisting of 6 'nests' of 3 concentric loops of pitch 5/36, 3/36 and 1/36 of the rotor circumference. Each nest offset by 1/6 of the circumference	
Rotor 2	Double layer winding of 18 successive single isolated turns each spanning 7/36 of the rotor circumference.	
Rotor 3	Novel double layer winding with 6 sets of 4 progressively wound groups of coils each coil spanning 1/6 of the rotor circumference, each set of coils is offset 1/6 of the circumference from the next, for full details see [16].	
Rotor 4	Conventional squirrel cage rotor as designed for the motor frame with Boucherot slot configuration.	

Alternative approaches include the two-phase model proposed by Broadway and Burbridge [4] and models derived from considerations of a three winding transformer [8]. Gorti et. al. use symmetrical component analysis applied to a coupled-circuit derived model [17]. A form of a single phase equivalent circuit has been presented, without derivation, by Liao [18].

Figure 8 shows the standard equivalent circuit for an induction motor with accessible rotor terminals, omitting iron losses. N is the effective turns ratio, L_m is the magnetizing inductance of the fundamental space harmonic field, as the equivalent circuit can only represent coupling between rotor and stator for one field component, in this case the fundamental. However the rotor and stator circuits must include series inductance terms which correspond to the additional series inductance due to any space harmonics created in the stator and rotor respectively. These terms appear in series with leakage terms, i.e. terms which represent the flux which self-links without crossing the air gap. On the stator the term L_1 includes both these harmonic terms and leakage terms. On the rotor L_r represents these terms.

If we now have two induction machines with different pole numbers, then we will have two induction motor equivalent circuits. These machines may share the same frame, and even the same iron circuit as the magnetic fields are of differing pole number (subject to conditions on the choice of pole number

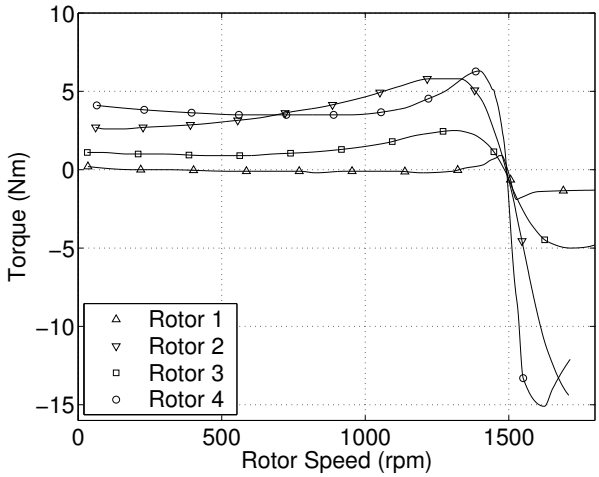

Fig. 4. Measured torque-speed characteristic, 4 pole stator supplied with 90Vrms, 8 pole stator open circuit ('simple induction mode').

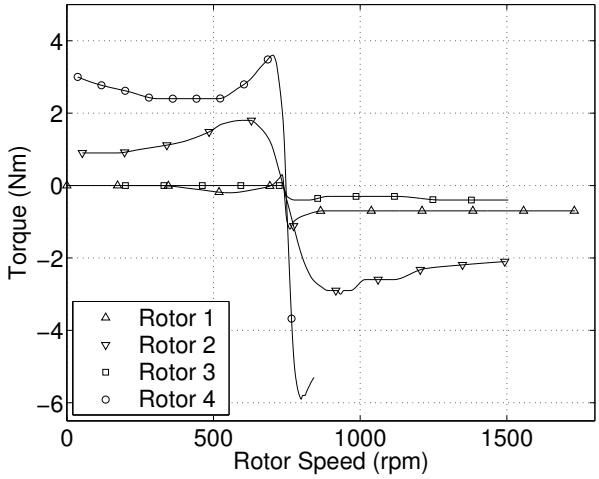

Fig. 5. Measured torque-speed characteristic, 8 pole stator supplied with 90Vrms, 4 pole stator open circuit ('simple induction mode').

to avoid unbalanced magnetic pull [19]). If each 'machine' has a wound rotor of the appropriate pole number, then the equivalent circuit parameters of each 'machine' have the same interpretation as those of figure 8.

Notice that each equivalent circuit would, in general, have its own slip, s_1 and s_2, as previously defined in (2), (3).

For an electrical machine to admit an equivalent circuit representation, the frequencies of the currents and voltages at the terminals must be equal. When the BDFM is operating in synchronous or cascade modes the rotor shaft speed and stator frequencies are related by (1), rearranging this gives:

$$\omega_{r_1} = \omega_1 - p_1\omega_r = -\omega_2 + p_2\omega_r = -\omega_{r_2} \quad (5)$$

$$\Rightarrow s_1\omega_1 = -s_2\omega_2 \quad (6)$$

where ω_{r_1} and ω_{r_2} are the frequencies of the field in the rotor reference frame, hence the rotor frequencies in the referred circuit are equal in magnitude.

Suppose that we now connect the two rotors together, as

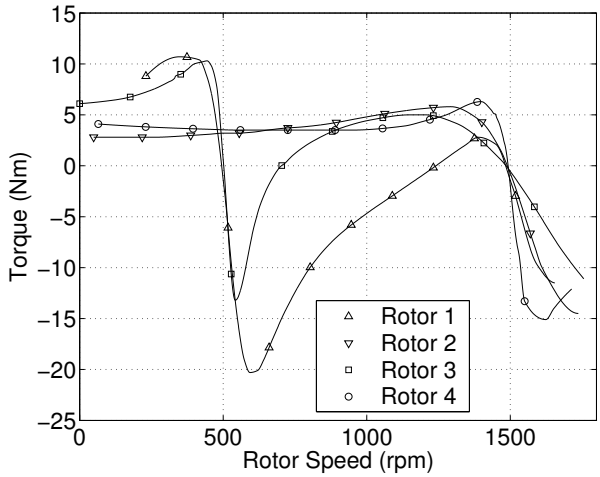

Fig. 6. Measured torque-speed characteristic, 4 pole stator supplied with 90Vrms, 8 pole stator short circuited ('cascade induction mode').

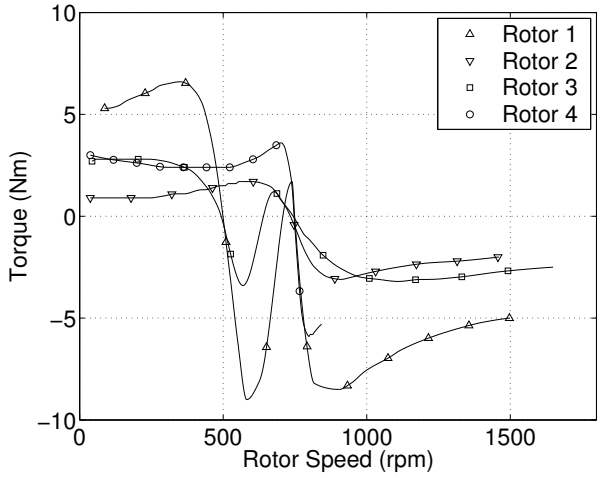

Fig. 7. Measured torque-speed characteristic, 8 pole stator supplied with 90Vrms, 4 pole stator short circuited ('cascade induction mode').

shown in figure 9. From (6) it can be seen that $j\omega_2 s_2 L_{r_2} = -j\omega_{r_2} L_{r_2}$, which is equivalent to reversing the direction of current flow, hence the current direction through transformer 2 in figure 9 must be opposite to that of figure 8. Furthermore we may combine the rotor resistance into a single term, R_r.

This representation of the equivalent circuit is correct for any functioning BDFM irrespective of rotor design. When the BDFM has a specially designed rotor winding, as per [11], the rotor inductance may be understood as follows: As the machine only has one rotor it is more natural to represent the rotor by a single resistance and a single reactance. As L_m consists purely of spatial harmonic inductance corresponding to the stator pole number, L_r must contain all other harmonic components. Since any functional BDFM rotor links stator 1 and stator 2 pole number fields, the magnetizing reactance for the stator 2 pole number field is contained within L_r, or more

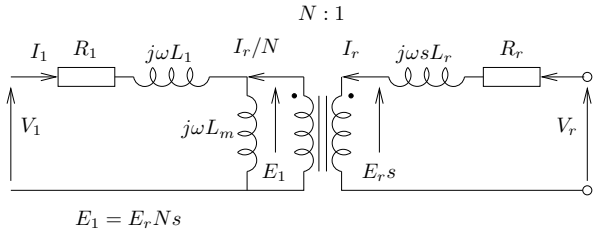

Fig. 8. Induction Machine Per-Phase Equivalent Circuit with Rotor Terminals

precisely:

$$L_r = L_{r_1} + L_{r_2} + \frac{L_{m_2}}{{N_2}^2} \tag{7}$$

if the stator 1 winding is supplied or

$$L_r = L_{r_1} + L_{r_2} + \frac{L_{m_1}}{{N_1}^2} \tag{8}$$

if stator 2 winding is supplied.

It follows that in a BDFM rotor the spatial harmonic component of the self-inductance contains harmonic components of both stator 1 and stator 2 pole number fields.

It may be noted that this cannot be achieved with a standard squirrel cage rotor as the harmonic inductance of a cage rotor depends on the 'supplied' field pole number. For example if stator 1 is 4 pole, then the cage rotor harmonic inductance only contains 4 pole (and higher harmonic) components. As there are no even harmonics, there is no 8 pole component. Therefore, figure 9 is not appropriate for a cage rotor.

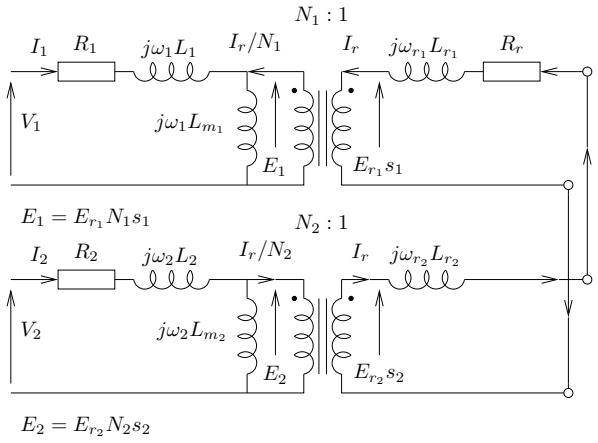

Fig. 9. BDFM Per-Phase Equivalent Circuit

In figure 9, R_1 and R_2 are the resistances of the stator windings and R_r is the rotor resistance. $j\omega_1 L_1$ and $j\omega_2 L_2$ are the stator reactances and $j\omega_r L_r$ is the rotor reactance. The power winding is linked to the rotor by a transformer of turns ratio N_1 and the control winding is linked by a transformer of turns ratio N_2, as shown. The secondary voltages of the transformers are proportional to slip and the slips are respectively s_1 and s_2 for the power and control windings.

As for the conventional induction motor, it is convenient to refer all quantities to the stator, as in figure 10 with values

referred to stator 1. Alternatively, it is possible to transfer values to stator 2.

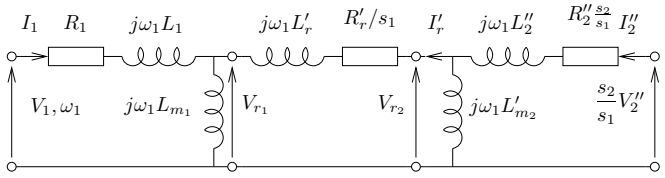

Fig. 10. Referred Per-Phase Equivalent Circuit

We can now find an expression for torque by considering how the conversion of electrical to mechanical energy is represented in the equivalent circuit. By applying the principle of power conservation to figure 10 we get:

$$3\Re\{V_1 I_1^*\} + 3\frac{s_2}{s_1}\Re\{V_2'' I_2''^*\} = 3|I_1^2|R_1 + 3|I_r'^2|\frac{R'_r}{s_1} + 3|I_2''^2|R''_2\frac{s_2}{s_1} \quad (9)$$

$$3\Re\{V_1 I_1^*\} + 3\Re\{V_2'' I_2''^*\} = 3|I_1^2|R_1 + 3|I_r'^2|R'_r + 3|I_2''^2|R''_2 + \omega_r T \quad (10)$$

where T is the torque generated by the machine, with positive values for motoring, and the '3's arise because figure 10 is a per-phase equivalent circuit.

From figure 10 we may define P_{r_1}, P_{r_2}, the power delivered at the rotor terminals from stator 1 and 2 respectively:

$$P_{r_1} \triangleq 3\Re\{V_{r_1} I_1^*\} = 3\Re\{V_1 I_1^*\} - 3|I_1^2|R_1 \quad (11)$$

$$P_{r_2} \triangleq 3\frac{s_1}{s_2}\Re\{V_{r_2} I_2''^*\} = 3\Re\{V_2'' I_2''^*\} - 3|I_2''^2|R''_2 \quad (12)$$

Subtracting (9) from (10) gives the fraction of power not dissipated in the rotor and stator resistances, i.e. the power which is converted to mechanical power:

$$3\Re\{V_2'' I_2''^*\}\left(1 - \frac{s_2}{s_1}\right) = 3|I_r'^2|R'_r\left(1 - \frac{1}{s_1}\right) + 3|I_2''^2|R'_2\left(1 - \frac{s_2}{s_1}\right) + \omega_r T \quad (13)$$

Rearranging, and substituting (12) for the I_2'' terms gives the torque as:

$$T = \frac{P_{r_2}}{\omega_r}\left(1 - \frac{s_2}{s_1}\right) - \frac{3}{\omega_r}|I_r'^2|R'_r\left(1 - \frac{1}{s_1}\right) \quad (14)$$

Referring back to the definition of BDFM synchronous speed (1), and slips (2), (3), it is straightforward to see that the rotor speed, ω_r can be written in terms of a deviation from natural speed, as defined in (4):

$$\omega_r = \left(1 - \frac{s_1}{s_2}\right)\omega_n \quad (15)$$

Using (15), (2) and (12) the expression for the torque, (14), may be succinctly written as:

$$T = -\frac{3\Re\{V_{r_2} I_2''^*\}}{\omega_n} + 3|I_r'^2|R'_r\frac{p_1}{\omega_1 s_1} \quad (16)$$

Under normal running conditions the power conversion is largely represented by $\frac{3\Re\{V_{r_2} I_2''^*\}}{\omega_n}$ term in equation (16) as slips are generally not small. In contrast to the cage rotor induction motor, power conversion could be achieved even if the rotor resistance were zero, as is the case in induction machines where the rotor circuit is externally fed via slip rings. It is in fact advantageous to reduce the rotor resistance as far as is practical to minimise losses.

VI. Equivalent Circuit Parameter Identification

The no load and locked rotor tests are the classical way of determining parameters for the equivalent circuit of the conventional induction motor. In the case of the BDFM the no load test can be applied in turn to each stator winding, with the other open circuit, to determine the magnetizing reactance. As the self-induction torque of a BDFM is likely to be relatively small, an external drive may be needed to run the machine at synchronous speed but in any case this will improve the accuracy of the measurements. Stator resistances can be found through DC measurements. However, the locked rotor test cannot be used to determine the remaining parameters individually. For example, the two components L'_r and L''_{m_2} cannot be separated. Although L_{m_2} may be determined using the synchronous test it is not possible to find the referred value, L''_{m_2} as the turns ratio is not known.

Recognising that the equivalent circuit can predict the behaviour of the machine in both simple induction and cascade modes, we propose an alternative approach based on the extraction of parameters from measured torque-speed characteristics of the kind shown in figures 4-7. This approach has the advantage that a single frequency supply may be used to perform the tests. This is in contrast to the only previously published works on BDFM parameter extraction, [20], [21], where a method requiring operation at a range of different supply frequencies is proposed.

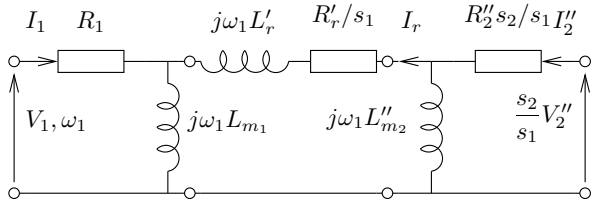

Fig. 11. Simplified Referred Per-Phase Equivalent Circuit

Nevertheless, not all the inductance terms in the equivalent circuit shown in fig. 10 can be unambiguously determined. An alternative form of the equivalent circuit is shown in fig. 11 for which all component values can be determined. A similar modification was proposed by Slemon in the case of parameter determination for the equivalent circuit for the standard induction motor [22]. For the circuit to be electrically equivalent to that of fig. 10 the parameters, and turns ratios, will assume slightly different values, which can easily be calculated, see appendix II. However, in a BDFM the referred series rotor inductance is likely to be larger than the series

stator inductance so differences in inductance values between the two circuits will be small. Direct measurements of rotor bar currents, for example using techniques described in [13], enable all parameters in fig. 10 to be determined, but the relationship of these currents to those in the equivalent circuit must be known.

The parameter extraction is a nonlinear optimisation method, using a weighted sum of the squares of the errors between predicted values and those measured by experiment as a cost function. A significant advantage over previous methods is that the machine is being tested under conditions similar to those found in normal operation. The parameter extraction and optimisation methods are described in full in appendix I.

The method was applied to the data of the kind shown in figures 4-7. Each data set had between 10 and 15 data points. When solving the optimization problem, in order to minimise the execution time of each random test point the mathematical functions governing the behaviour of the machine were simplified as far as possible using the symbolic maths package, Maple, and then hard coded in a C function along with the random number generation code. This function was then called from Matlab. With this implementation it was possible, using a 2.8GHz Pentium processor,to achieve 4×10^5 tests per second in cascade mode and slightly more in simple mode.

As an indication of the time taken to solve the optimization to satisfactory accuracy, it took approximately 9×10^8 tests taking around 40 minutes to generate 10 candidate solutions of suitable accuracy for rotor 1. Tables II, III and IV show the results of 2×10^{10} tests, along with the standard deviation taken over the best 20 results. The standard deviations are generally considerably smaller than the estimated parameter values, which indicates that the noise level in the measurements is sufficiently low to have confidence in the results. As an additional measure of effectiveness the algorithm returns the value of the minimised error which, if suitably normalised, gives a measure of fit 'quality'.

Parameters obtained from tests in the simple induction mode are given in Table II with the 4-pole winding excited; the tests can be performed equally well by energizing the 8-pole winding. The substantial values of the referred magnetizing inductance ($L''_{m_2}\frac{N_2}{N_1}$) with Rotors 1 and 3 reflect effective cross-coupling, and explain the high value of effective referred rotor inductance ($L'_r + L''_{m_2}$). In contrast Rotor 2 shows very weak cross-coupling; Rotor 4, the conventional cage rotor, shows no measurable cross-coupling, and the corresponding effective referred rotor inductances are correspondingly smaller. Therefore it is only possible to obtain meaningful parameters in the cascade mode for Rotors 1 and 3 and these are given in tables III and IV for 4-pole and 8-pole excitation respectively. Similar values are obtained in both cases, and the values are reasonably consistent with the values found from simple induction mode tests.

Manufacturer's data are available for Rotors 2 and 4. Allowing for differences in air gap dimensions, inductance values are in the expected range. However, values of rotor resistance can be directly compared and the manufacturer gives 1.28Ω and 0.46Ω for Rotors 2 and 4 respectively. The closeness of these values to those given in Table II confirm the effectiveness of this method of parameter determination.

TABLE II
SIMPLE INDUCTION MODE EXTRACTED PARAMETER VALUES 4 POLE WINDING

	R_1 (Ω)	R'_r (Ω)	$L'_r + L''_{m_2}$ (mH)	L_{m_1} (mH)	$L''_{m_2}\frac{N_2}{N_1}$ (mH)
Rotor 1: nested-loop rotor design					
Opt:	4.02	1.2	120	240	137
Std. Dev.:	0.0243	0.00769	0.204	0.0507	0.00879
Rotor 2: 18 isolated loops rotor design					
Opt:	3.28	1.36	26.1	252	5.46
Std. Dev.:	0.0548	0.00627	0.199	5.19	0.00855
Rotor 3: new double-layer rotor design					
Opt:	3.52	3.1	65.5	260	105
Std. Dev.:	0.0384	0.0306	0.246	4.44	0.547
Rotor 4: standard cage rotor design					
Opt:	3.54	0.486	22.8	253	0
Std. Dev.:	0.049	0.00705	0.202	17.7	0

TABLE III
CASCADE INDUCTION MODE EXTRACTED PARAMETER VALUES 4 POLE WINDING

	R_1 (Ω)	R'_r (Ω)	L'_r (mH)	L_{m_1} (mH)	R''_2 (Ω)	L''_{m_2} (mH)	$\frac{N_1}{N_2}$
Rotor 1: nested-loop rotor design							
Opt:	3.63	1.26	35.1	277	2.46	101	0.685
Std. Dev.:	0.106	0.038	0.379	27.1	0.0628	3.83	0.0131
Rotor 3: new double-layer rotor design							
Opt:	3.6	2.92	27.4	299	0.716	40.8	0.408
Std. Dev.:	0.125	0.0673	0.386	32.8	0.0197	1.55	0.00788

In the extraction of the parameters, the solver aimed for a best fit of all parameters. Alternatively, certain parameters which can be accurately determined by independent means can be fixed. These include the sum of L_1 and L_m, which can be obtained from a synchronous or no load test, and the stator winding resistances which can be obtained from DC measurements at working temperature, assuming that the skin effect can be ignored in the staor windings.

VII. RESULTS VERIFICATION OF PREDICTIONS FROM THE EQUIVALENT CIRCUIT

To demonstrate the use of the equivalent circuit, it has been used to predict the performance of the BDFM in both synchronous and cascade (asynchronous) modes. Figure 12 shows a torque-speed curve for Rotor 3. The machine 4 pole stator winding was supplied with a constant voltage and frequency supply at 90V and 50 Hz. The machine 8 pole winding was short-circuited, hence the machine was operaing

TABLE IV
CASCADE INDUCTION MODE EXTRACTED PARAMETER VALUES 8 POLE WINDING

	R_1 (Ω)	R'_r (Ω)	L'_r (mH)	L_{m_1} (mH)	R''_2 (Ω)	L''_{m_2} (mH)	$\frac{N_1}{N_2}$
Rotor 1: nested-loop rotor design							
Opt:	5.79	2.82	72.9	288	7.25	391	1.41
Std. Dev.:	0.213	0.0951	0.919	19.5	0.28	25.5	0.0447
Rotor 3: new double-layer rotor design							
Opt:	5.39	23.5	189	281	22.9	1640	2.51
Std. Dev.:	0.391	0.377	1.27	5.52	0.487	39.4	0.0301

in *cascade induction* mode. The figure shows experimental points overlaid with a calculated torque-speed curve generated from the parameters listed in table III using the equivalent circuit in figure 11. Negative torque denotes that the machine is acting as a generator. Close agreement between predicted and measured values is seen.

Figure 13 shows a synchronous torque envelope for Rotor 3, with experimental data points overlaid. Again, the machine 4 pole stator winding was supplied from a constant voltage and frequency supply at 90V and 50 Hz. However the machine 8 pole stator winding was fed with a variable voltage, variable frequency supply of f_2 Hz at $230 \times (f_2/50)$V. Again there is good agreement between theory and experiment. The dip in the torques near 500 rpm could have been overcome by applying a suitable voltage boost to the 8 pole stator winding at low excitation frequencies to maintain a constant voltage $|V_{r_2}|$.

Figure 14 shows a synchronous torque envelope for Rotor 1 with a higher voltage (220 V) applied to the 4 pole stator winding. The 8 pole stator winding was supplied with a variable voltage, variable frequency supply of f_2 Hz at at $220 \times (f_2/50)$V, with a voltage boost below $f_2 = 5$Hz. However, there is still a dip in torque near 500 rpm, arising the change in sign of the voltage across the stator impedance. The torque envelope can be flattened by applying a voltage boost which is slightly asymmetrical about natural speed (500 rpm). The absence of measurements of generating torque above 100 Nm arises from limitations of the external drive.

VIII. CONCLUSIONS

We have presented experimental torque speed characteristics from a BDFM equipped with four rotor variants. A per phase equivalent circuit valid for all modes of operation has been developed. The circuit parameters have precise physical meanings and torque equations have been derived. With a simple modification the circuit reduces to a form for which all parameters can be obtained experimentally. A method of determining these parameters from measurements at machine terminals is presented. The equivalent circuit has been used to predict torque-speed characteristics in both synchronous and cascade modes and these predictions are in good agreement with measured values.

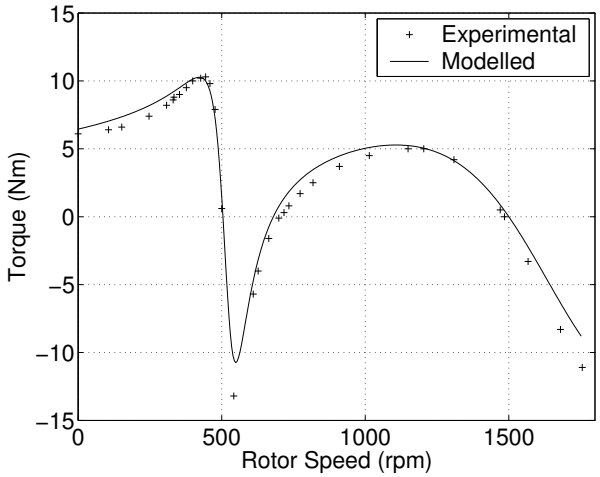

Fig. 12. Experimental verification of the parameter extraction procedure: A torque-speed plot for rotor 3 with the 4 pole winding supplied with nominally 90V (phase). The 8 pole winding is short-circuited. The continuous line is generated with previously extracted parameters as shown in table III

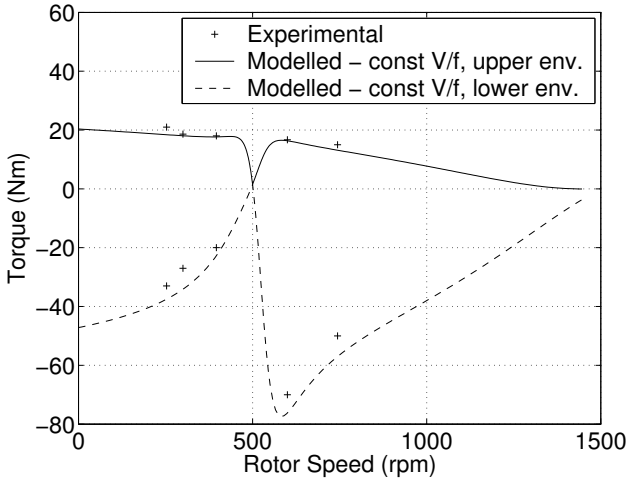

Fig. 13. Experimental verification of the parameter extraction procedure: Synchronous torque envelope with varying rotor speed for rotor 3 with the 4 pole winding supplied with nominally 90V (phase), the 8 pole is supplied with $2.56 \times 90\frac{f_2}{f_1}$ (predicted: solid and dashed lines, experimental points marked). The parameters values used are those of table III.

The performance of the rotors for a BDFM can be related to their equivalent circuit parameters. Although a full comparison is beyond the scope of this paper, we can note that the torque envelope depends strongly on the referred rotor resistance and reactance. A good rotor design will therefore involve making R'_r and L'_r as low as practical. Reducing L'_r is particularly challenging as harmonic inductance components are likely to be dominant. The harmonic elements are a consequence of the need to couple fields of different pole numbers and can only be minimized by careful rotor design.

The method of parameter estimation is geared to finding equivalent circuit values which give predictions that closely match the observed behaviour of the machine. We are currently looking at effects of saturation on parameter values and

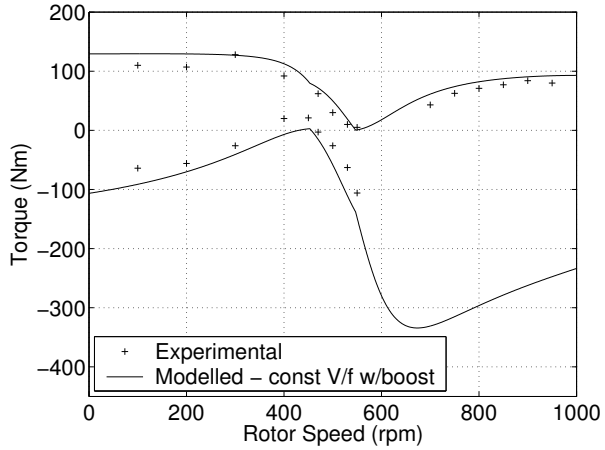

Fig. 14. Experimental verification of the parameter extraction procedure: Maximum synchronous torque envelope with varying rotor speed for rotor 1 ('nested-loop' design) with the 4 pole winding supplied with nominally 220V (phase), the 8 pole is supplied with a const. V/f law with boost, i.e.: $V_8 = \max\{220\left|\frac{f_2}{f_1}\right|, 20.7\}$ (solid lines, with experimental points marked). The parameters values used are those of table III.

whether accurate prediction of machine performance will remain possible. In addition, the method of parameter estimation can be used to find values for the equivalent circuit of the standard induction motor.

ACKNOWLEDGEMENTS

The authors wish to thank FKI Energy Technology, particularly its subsidiaries (Laurence, Scott & Electromotors Ltd. and Marelli Motori SpA) for their continued support, particularly for the provision of the prototype machine and fabrication of the rotors. Semikron UK Ltd. is thanked for supplying an inverter.

APPENDIX I
PARAMETER EXTRACTION OPTIMIZATION METHOD

A. General Optimisation Problem

The optimisation problem to be solved is a non-linear least squares problem, and can be stated as:

Given $Y_i \in \mathbb{R}^k$, $P \in \mathbb{R}^n$, $U \in \mathbb{R}^{k\times m}$, $F_i : P, U \mapsto \mathbb{R}^k$, $i \leq l$

$$\text{Find} \quad P : \min_{P\in W\mathbb{B}+P_0} \sum_{i=1}^{l} S_i \|Y_i - F_i(P,U)\|_2 \qquad (17)$$

where F_i is a function which estimates the i^{th} measured output for a particular parameter vector, P. U is a matrix of input data points where each row is an individual data point. Y_i is a vector of the measured i^{th} output data due to U. There are k input/output data pairs and m different measured outputs (i.e. U has k rows and m columns). S_i is a scalar weight applied to the i^{th} output error. So there are n parameters, m inputs, k data points for each input, and l outputs. Furthermore, F_i is defined as:

$$F_i(P,U) = \begin{bmatrix} f_i(P,u_1) \\ \vdots \\ f_i(P,u_k) \end{bmatrix}, \qquad U = \begin{bmatrix} u_1 \\ \vdots \\ u_k \end{bmatrix} \qquad (18)$$

where $f_i : P, u_j \mapsto \mathbb{R}^1$.

$W\mathbb{B} + P_0$ represents the set of possible parameter values which is chosen from a rectangular set (as $\mathbb{B}$ is a hypercube), centred on P_0 with corners at $P_0 \pm \text{diag}(W)$. Clearly the value of P that gives the minimum cost function value will, in general, not be unique. As stated this is a non-convex optimization problem, and therefore difficult to solve [23].

In order to solve this optimisation problem we use a simple (or crude) random search (also known as a 'Monte Carlo' method). For practical and theoretical details of the algorithm see, for example, [23]. The principal advantage of a simple random search, for our purposes, is its strong resilience to measurement noise and modelling error while guaranteeing convergence to the global minimum. Furthermore because it requires no gradient information there is no need for any a priori information about the particular cost function, and it can be shown that without any such information then a simple random search is as efficient as any other method, in reaching the global minimum [24]. The simplicity of the algorithm means that implementation is straightforward, and because the method does not depend on the cost function chosen, the algorithm can be applied to different cost functions without modification.

The search is performed across $W\mathbb{B} + P_0$ to find $Q = \{q_1, \cdots, q_N\}$ where $Q : \sum_{i=1}^{m} S_i \|Y_i - F_i(q,U)\|_2 \leq \gamma$, where $\gamma > 0$ is an acceptable value for the cost function to take. We generate guesses for candidate q_ks using the Mersenne Twister [25], a fast uniform random number generator with a long repetition period. Having found Q we then find the, q_k corresponding to the minimum cost, K_{min}. This q_k, called q_{opt} henceforth is an estimate of the global minimizer and K_{min} an estimation of the global minimum. Furthermore the standard deviation of Q gives an indication of how much confidence one should have in taking q_{opt} as the global minimum.

Although the efficiency could be increased by using a multi-start, (see [23] for details) or probabilistic branch and bound algorithm (such as [26]), the additional complexity of the algorithm, and requirements to have some appreciation of the modelling error and noise, make these algorithm less appealing than they might first appear. Furthermore there is a tradeoff between increased complexity in the algorithm versus the decreased number of iterations required.

B. Application to BDFM

Notice that thus far it has not been necessary to specify *what* the measured outputs, Y are, or what the estimation functions F are.

We desire to choose the inputs and output such that they are easy to measure 'terminal' quantities. Therefore we are restricted to the stator voltages, currents, the torque and the rotor speed. Furthermore due to the substantial difficulty

of trying to measure the phase difference between stator 1 and stator 2 quantities we restrict ourselves to magnitude measurements of stator 2 quantities.

In *simple induction* mode operation there are 2 inputs, 3 measured outputs, 4 parameters, and N_s data points. The subscript simple/1 is used to indicate simple induction mode referred to stator 1. Y is chosen as follows:

$$Y_{\text{simple/1}_1} = \begin{bmatrix} T_1 \\ \vdots \\ T_k \end{bmatrix}, \qquad Y_{\text{simple/1}_2} = \begin{bmatrix} \Re\{I_{1_1}\} \\ \vdots \\ \Re\{I_{1_k}\} \end{bmatrix} \tag{19}$$

$$Y_{\text{simple/1}_3} = \begin{bmatrix} \Im\{I_{1_1}\} \\ \vdots \\ \Im\{I_{1_k}\} \end{bmatrix}, \quad U_{\text{simple/1}} = \begin{bmatrix} \omega_{r1} & V_{1_1} \\ \vdots & \vdots \\ \omega_{rk} & V_{1_k} \end{bmatrix} \tag{20}$$

$$P_{\text{simple/1}} = \begin{bmatrix} R_1 \\ R'_r \\ L'_r + L''_{m_2} \\ L_{m_1} \end{bmatrix} \tag{21}$$

$F_{\text{simple/1}_i}$ can be derived from the referred equivalent circuit, figure 11, taking $I''_2 = 0$:

$$T = f_{\text{simple/1}_1}(P_{\text{simple/1}}, u_{\text{simple/1}}) \tag{22}$$

$$\Re\{I_1\} = f_{\text{simple/1}_2}(P_{\text{simple/1}}, u_{\text{simple/1}}) \tag{23}$$

$$\Im\{I_1\} = f_{\text{simple/1}_3}(P_{\text{simple/1}}, u_{\text{simple/1}}) \tag{24}$$

If $U_{\text{simple/1}_1}$ is chosen so that the BDFM is exercised over a range of speeds such that the slip (2) varies substantially, say from 0 to 1.5, it can be shown from the equivalent circuit that each $f_{\text{simple/1}_i}$ depends strongly on each element of $P_{\text{simple/1}}$, therefore there is a unique $P_{\text{simple/1}}$ which solves the optimization problem. However due to the presence of measurement noise and modelling error this will not necessarily be the case. Solving this optimization problem as outlined in section I-A gives the parameters indicated in (21).

However we have not used $|V_2|$ as one of the measurable outputs. It can be seen from figure 11, with $V''_2 = V_2 \frac{N_1}{N_2}$ (from figure 9):

$$|V_2|\frac{N_1}{N_2} = |I'_r \omega_1| L_{m_2} \tag{25}$$

and the ratio of the turns ratios, $\frac{N_1}{N_2}$ is unknown. Therefore all that can be achieved is the determination of $\frac{N_2}{N_1} L_{m_2}$. It is proposed therefore that, having determined the optimal parameter set, linear least-squares is used to determine $\frac{N_2}{N_1} L_{m_2}$:

$$\frac{N_2}{N_1} L_{m_2} = A^T (A^T A)^{-1} \begin{bmatrix} |I'_{r_1} \omega_{1_1}| \\ \vdots \\ |I'_{r_k} \omega_{1_k}| \end{bmatrix}, \quad A = \begin{bmatrix} |V_{2_1}| \\ \vdots \\ |V_{2_k}| \end{bmatrix}$$

and $|I'_{r_j}|$ are calculated from figure 11 using the optimal parameter set.

In *cascade induction* mode operation there are 2 inputs, 4 measured outputs, 6 parameters, and N_c data points. The subscript cascade/1 is used to indicate simple induction mode referred to stator 1. Y is chosen as follows:

$$Y_{\text{cascade/1}_1} = \begin{bmatrix} T_1 \\ \vdots \\ T_k \end{bmatrix}, \qquad Y_{\text{cascade/1}_2} = \begin{bmatrix} \Re\{I_{1_1}\} \\ \vdots \\ \Re\{I_{1_k}\} \end{bmatrix} \tag{26}$$

$$Y_{\text{cascade/1}_3} = \begin{bmatrix} \Im\{I_{1_1}\} \\ \vdots \\ \Im\{I_{1_k}\} \end{bmatrix}, \qquad Y_{\text{cascade/1}_4} = \begin{bmatrix} |I_{2_1}| \\ \vdots \\ |I_{2_k}| \end{bmatrix} \tag{27}$$

$$U_{\text{cascade/1}} = \begin{bmatrix} \omega_{r1} & V_{1_1} \\ \vdots & \vdots \\ \omega_{rk} & V_{1_k} \end{bmatrix}, \qquad P_{\text{cascade/1}} = \begin{bmatrix} R_1 \\ R'_r \\ L'_r \\ L'_{m_1} \\ R''_2 \\ \frac{N_1}{N_2} \end{bmatrix} \tag{28}$$

$F_{\text{simple/1}_i}$ can be derived from the referred equivalent circuit, figure 11, taking $V''_2 = 0$:

$$T = f_{\text{simple/1}_1}(P_{\text{simple/1}}, u_{\text{simple/1}}) \tag{29}$$

$$\Re\{I_1\} = f_{\text{simple/1}_2}(P_{\text{simple/1}}, u_{\text{simple/1}}) \tag{30}$$

$$\Im\{I_1\} = f_{\text{simple/1}_3}(P_{\text{simple/1}}, u_{\text{simple/1}}) \tag{31}$$

$$|I_2| = f_{\text{simple/1}_4}(P_{\text{simple/1}}, u_{\text{simple/1}}) \tag{32}$$

As for the simple mode $U_{\text{cascade/1}_1}$ is chosen so that the BDFM is exercised over a range of speeds such that the slip (2) varies substantially, it can be shown from the equivalent circuit that each $f_{\text{cascade/1}_i}$ depends strongly on each element of $P_{\text{cascade/1}}$. However $f_{\text{cascade/1}_i}$ also depends on L_2, and it is not possible to determine this from the measured outputs. Therefore the value extracted from the simple/2 is used, and is explicitly included in $f_{\text{cascade/1}_i}$. In these circumstances there is a unique $P_{\text{cascade/1}}$ which solves the optimization problem, with the same caveat regarding noise and measurement error as in the simple mode procedure. Again the optimization problem is solved as outlined in section I-A giving the parameters indicated in (28).

Although the original problem (17) contained S_i, a weight, it is set to unity without exception for the applications described. The choice of weight can improve the algorithm by compensating for different scaling of the measured outputs, for example if $|V_2|$ had been included as a measured output then it would have been appropriate to scale down the effect of the error on this measurement as it is typically 2 orders of magnitude larger than the other measured outputs.

APPENDIX II
EQUIVALENT NETWORKS

Figure 15 shows equivalent forms of the 'T' and 'Γ' networks, details can be derived using, for example, [27].

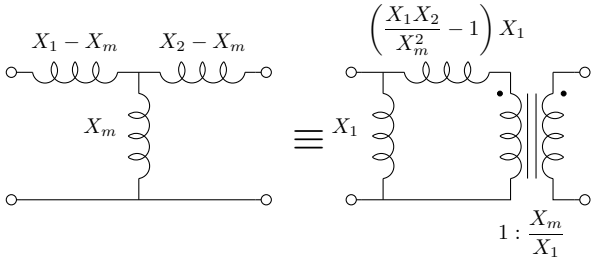

Fig. 15. Equivalent forms of 'T' and 'Γ' networks

REFERENCES

[1] Siemens Brothers & Co. Ltd. and F. Lydall, "Improvements in polyphase induction motors," British Patent No.: 16839, July 1902.

[2] L. J. Hunt, "A new type of induction motor," *Institution of Electrical Engineers, Journal*, pp. 648–677, 1907.

[3] ——, "The 'cascade' induction motor," *Institution of Electrical Engineers, Journal*, pp. 406–434, 1914.

[4] A. R. W. Broadway and L. Burbridge, "Self-cascaded machine: a low-speed motor or high frequency brushless alternator," *Proceedings, Institution of Electrical Engineers*, vol. 117, pp. 1277–1290, 1970.

[5] A. K. Wallace, P. Rochelle, and R. Spée, "Rotor modelling and development for brushless doubly-fed machines," in *Conference record of the International Conference on Electrical Machines*, vol. 1. Cambridge,MA: ICEM, August 12-15 1990.

[6] R. Li, A. Wallace, and R. Spée, "Two-axis model development of cage-rotor brushless doubly-fed machines," *IEEE Transactions on Energy Conversion*, vol. 6, no. 3, pp. 453–460, 1991.

[7] ——, "Dynamic simulation of brushless doubly-fed machines," *IEEE Transactions on Energy Conversion*, vol. 6, no. 3, pp. 445–452, 1991.

[8] R. Li, R. Spée, A. K. Wallace, and G. C. Alexander, "Synchronous drive performance of brushless doubly-fed motors," *IEEE Transactions on Industry Applications*, vol. 30, no. 4, pp. 963–970, July/August 1994.

[9] M. Boger, A. Wallace, R. Spée, and R. Li, "General pole number model of the brushless doubly-fed machine," *IEEE Transactions on Industry Applications*, vol. 31, no. 5, pp. 1022–1028, 1995.

[10] M. Boger, A. Wallace, and R. Spée, "Investigation of appropriate pole number combinations for brushless doubly fed machines as applied to pump drives," *IEEE Transactions on Industry Applications*, vol. 31, no. 5, pp. 1022–1028, 1996.

[11] S. Williamson, A. C. Ferreira, and A. K. Wallace, "Generalised theory of the brushless doubly-fed machine. part 1: Analysis," *IEE Proceedings - Electric Power Applications*, vol. 144, no. 2, pp. 111–122, 1997.

[12] S. Williamson and A. C. Ferreira, "Generalised theory of the brushless doubly-fed machine. part 2: Model verification and performance," *IEE Proceedings - Electric Power Applications*, vol. 144, no. 2, pp. 123–129, 1997.

[13] P. C. Roberts, E. Abdi-Jalebi, R. A. McMahon, and T. J. Flack, "Real-time rotor bar current measurements using bluetooth technology for a brushless doubly-fed machine (BDFM)," in *Int. Conf. Power Electronics, Machines and Drives (PEMD)*, vol. 1. IEE, March 2004, pp. 120–125.

[14] E. Abdi-Jalebi, P. C. Roberts, and R. A. McMahon, "Real-time rotor bar current measurement using a rogowski coil transmitted using wireless technology," in *18th Intl. Power Systems Conf. (PSC2003), Iran*, vol. 5, October 2003, pp. 1–9.

[15] P. C. Roberts, T. J. Flack, J. M. Maciejowski, and R. A. McMahon, "Two stabilising control strategies for the brushless doubly-fed machine (BDFM)," in *Int. Conf. Power Electronics, Machines and Drives (PEMD) (Conf. Pub. No. 487)*. IEE, 4-7 June 2002, pp. 341–346, bath, UK.

[16] P. C. Roberts, R. A. McMahon, P. J. Tavner, J. M. Maciejowski, T. J. Flack, and X. Wang, "Performance of rotors for the brushless doubly-fed (induction) machine (BDFM)," in *Proc. 16th Int. Conf. Electrical Machines (ICEM)*, September 2004, pp. 450–455, 5th-8th, Cracow, Poland.

[17] B. V. Gorti, G. C. Alexander, and R. Spée, "Power balance considerations for brushless doubly-fed machines," *IEEE Transactions on Energy Conversion*, vol. 11, no. 4, pp. 687–692, December 1996.

[18] Y. Liao, "Design of a brushless doubly-fed induction motor for adjustable speed drive applications," in *Proc. IEEE Industry App. Soc. Annual Mtg.* IEEE, 6-10 October 1996, pp. 850–855.

[19] F. Creedy, "Some developments in multi-speed cascade induction motors," *Institution of Electrical Engineers, Journal*, pp. 511–537, 1920.

[20] A. Ramchandran, G. C. Alexander, and R. Spée, "Off-line parameter estimation for the doubly-fed machine," in *Proceedings of Conference on Industrial Electronics, Control, Instrumentation, and Automation, 1992. 'Power Electronics and Motion Control'*, vol. 3. IEEE, 1992, pp. 1294–1298, 9-13 Nov 1992.

[21] A. Ramchandran and G. C. Alexander, "Frequency-domain parameter estimations for the brushless doubly-fed machine," in *Conference Record of PCC 1993*. Power Conversion Conference, Yokohama 1993: IEEE, 1993, pp. 346–351, 19-21 Apr 1993.

[22] G. R. Slemon, "Modelling of induction machines for electric drives," in *Conference record of the IEEE Industry Applications Society Annual Meeting*, vol. 1. IEEE, October 7-12 1989, pp. 111–115.

[23] A. A. Zhigljavsky, *Theory of Global Random Search*. Kluwer Academic Publishers, 1991.

[24] Y. C. Ho and D. L. Pepyne, "Simple explanation of the no-free-lunch theorem and its implications," *J. of Optimization Theory and Applications*, vol. 115, no. 3, pp. 549–570, December 2002.

[25] M. Matsumoto and T. Nishimura, "Mersenne twister: A 623-dimensionally equidistributed uniform pseudorandom number generator," *ACM Trans. on Modeling and Computer Simulation*, vol. 8, no. 1, pp. 3–30, January 1998, http://www.math.sci.hiroshima-u.ac.jp/ m-mat/eindex.html.

[26] Z. B. Tang, "Adaptive partitioned search to global optimization," *IEEE Transactions on Automatic Control*, vol. 39, no. 11, pp. 2235–2244, November 1994.

[27] A. B. Carlson, *Circuits: Engineering Concepts and Analysis of Linear Electric Circuits*. John Wiley & Sons Inc., New York, 1996.